Petroleum Science 22 (2025) 3042–3055

Contents lists available at ScienceDirect

Petroleum Science

journal homepage: www.keaipublishing.com/en/journals/petroleum-science

Original Paper

Hybrid deep learning framework with spatiotemporal pattern extraction for decant oil solid content soft sensor development in fluid catalytic cracking units

Nan Liu, Chun-Meng Zhu, Yu-Hui Li, Yun-Peng Zhao, Xiao-Gang Shi, Xing-Ying Lan *

State Key Laboratory of Heavy Oil Processing, China University of Petroleum (Beijing), Beijing, 102249, China

ARTICLE INFO

Article history:
Received 27 October 2024
Received in revised form
28 February 2025
Accepted 2 April 2025
Available online 4 April 2025

Edited by Min Li

Keywords:
Fluid catalytic cracking unit
Soft sensor
Deep learning
Shapley value
Risk identification

ABSTRACT

Coking at the fractionating tower bottom and the decant oil circulation system disrupts the heat balance, leading to unplanned shutdown and destroying the long period stable operation of the Fluid Catalytic Cracking Unit (FCCU). The FCCU operates through interconnected subsystems, generating high-dimensional, nonlinear, and non-stationary data characterized by spatiotemporally correlated. The decant oil solid content is the crucial indicator for monitoring catalyst loss from the reactor-regenerator system and coking risk tendency at the fractionating tower bottom that relies on sampling and laboratory testing, which is lagging responsiveness and labor-intensive. Developing the online decant oil solid content soft sensor using industrial data to support operators in conducting predictive maintenance is essential. Therefore, this paper proposes a hybrid deep learning framework for soft sensor development that combines spatiotemporal pattern extraction with interpretability, enabling accurate risk identification in dynamic operational conditions. This framework employs a Filter-Wrapper method for dimensionality reduction, followed by a 2D Convolutional Neural Network (2DCNN) for extracting spatial patterns, and a Bidirectional Gated Recurrent Unit (BiGRU) for capturing long-term temporal dependencies, with an Attention Mechanism (AM) to highlight critical features adaptively. The integration of SHapley Additive exPlanations (SHAP), Complementary Ensemble Empirical Mode Decomposition with Adaptive Noise (CEEMDAN), 2DCNN, and expert knowledge precisely quantifies feature contributions and decomposes signals, significantly enhancing the practicality of risk identification. Applied to a China refinery with processing capacity of 2.80×10^6 t/a, the soft sensor achieved the R^2 value of 0.93 and five-level risk identification accuracy of 96.42%. These results demonstrate the framework's accuracy, robustness, and suitability for complex industrial scenarios, advancing risk visualization and management.

1. Introduction

Fluid Catalytic Cracking Unit (FCCU) is a crucial technology in refining for both energy efficiency and stable production. Refineries are realizing the vision of an efficient, safe, and environmentally friendly industry through digital and intelligent transformation (Wu et al., 2024). However, FCCU is the highly complex installation, with multiple operation units, multi risk coupling characteristics, and the potential source of major hazards (Mkrtchyan et al., 2022). Due to the tightly coupled correlation among subsystems, deteriorating abnormal conditions can escalate safety risks and lead to unplanned shutdowns, disrupting long period stable operation and resulting in economic losses (Agarwal et al., 2022; Leveson and Stephanopoulos, 2014). Creating an appropriate balance between safety and economic goals has always been the focus of refineries (He et al., 2024; Liu et al., 2024). The coking failures degrade operating conditions, progressively reducing decant oil circulation and steam output, causing pipeline blockages, darkening diesel oil color, and ultimately limiting product quality and increasing safety risks. Decant oil solid content primarily results from catalyst loss in the reactor-regenerator system and coke formation in the fractionating tower bottom and decant oil circulation system. Catalyst fines enter the decant oil, increasing coking centers, while catalyst particles in high-temperature environments act as nucleation sites, accelerating the polymerization of polycyclic

* Corresponding author.
E-mail address: lanxy@cup.edu.cn (X.-Y. Lan).
Peer review under the responsibility of China University of Petroleum (Beijing).

https://doi.org/10.1016/j.petsci.2025.04.006

aromatic hydrocarbons, resins, and asphaltenes. Therefore, any increase in decant oil solid content-whether from catalyst or coke particles-signals the elevated coking risk tendency in the system. Due to technical and economic constraints, decant oil solid content cannot be directly measured by hardware sensors and rely instead on manual, offline lab analyses, causing time delays. This approach fails to meet the FCCU's requirement for real-time risk monitoring, which necessitates immediate integration of fundamental process mechanisms and risk factors to construct the soft sensor, enabling proactive intervention and ensuring safe production.

The advancement of instrumentation and automation technology in refineries generates comprehensive operational data, essential for the soft sensor development (Fisher et al., 2020). Soft sensors, critical for advanced process control, optimization, and monitoring, provide real-time online estimations of difficult-to-measure variables by leveraging correlations with easily measurable process variables (Kadlec et al., 2009). This overcomes limitations such as low sampling rates and offline risk monitoring, particularly valuable in FCCU applications due to resilience against predictive maintenance (Sun and Ge, 2021). Data-driven soft sensors, utilizing operational data from Distributed Control Systems (DCS) and Laboratory Information Management Systems (LIMS), offer a more precise representation of real-time operational conditions in FCCU (Ferreira et al., 2022). However, the industrial data of FCCUs is characterized by high-dimensional, nonlinear, and non-stationary, necessitating advanced feature extraction techniques to capture coupled spatiotemporal relationships. Traditional data-driven methods, such as Principal Component Analysis (PCA) and Artificial Neural Networks (ANN), are constrained by shallow architectures, limiting their capacity to extract complex, nonlinear patterns in large-scale processes under fluctuating operational conditions, resulting in lower convergence and generalizability (Perera et al., 2023).

Capturing spatiotemporal correlations through hybrid Deep Learning (DL) methodologies in soft sensor development is crucial for enhancing predictive accuracy, thereby maintaining process safety and product quality (Y. Z. Liu et al., 2024; Wang et al., 2024). Hybrid architectures integrating DL techniques like the Convolutional Neural Network (CNN), Long Short Term Memory Network (LSTM), and Attention Mechanism (AM) (Qin and Zhao, 2022) enhance the risk management across applications, including gas leakage detection (Kopbayev et al., 2022) and chemical process fault diagnosis (Arunthavanathan et al., 2021), by leveraging multiscale spatiotemporal dependencies for robust performance. The final premise of risk management involves identifying potential risk factors and consequences, enabling predictive and prescriptive strategies to improve the decision-making process and prevent accidents. While hybrid modeling techniques achieve credible results in industrial prediction tasks, their inherent 'black-box' nature remains the limitation in risk monitoring, where model transparency is essential for effective risk management (Zhang et al., 2024). The eXplainable Artificial Intelligence (XAI) has emerged for addressing interpretability challenges (Bhakte et al., 2022), with SHapley Additive exPlanation (SHAP) analysis offering notable post-hoc insights, that improve understanding of model intrinsic decision-making mechanisms (Sharma Timilsina et al., 2024). Integrating SHAP analysis with the decant oil solid content soft sensor enables operators to handle the coking anomaly at the fractionating tower bottom while identifying critical risk factors, thus supporting subsequent risk identification through signal decomposition. The convergence of signal processing and DL techniques provides a robust framework for continuous risk identification (Cui et al., 2024). High-frequency signals, such as flow and temperature, are valuable due to their rich operational information across extensive time scales; these signals are meticulously analyzed in the time-frequency domain to detect fluctuating operational conditions in FCCUs. Numerous studies have been dedicated to characterizing the features contained in these signals (Liu et al., 2020). Signal processing methods, including time-frequency domain analysis, Empirical Mode Decomposition (EMD) (Yuzgec et al., 2024), Ensemble Empirical Mode Decomposition (EEMD) (Xue et al., 2024), and Complementary Ensemble Empirical Mode Decomposition with Adaptive Noise (CEEMDAN) (Kim et al., 2022), have demonstrated remarkable success in signal decomposition. This integrated approach harnesses the strengths of both signal processing and DL techniques, enabling automated and high-accuracy risk identification and adaptation in complex industrial scenarios.

In conclusion, the decant oil solid content soft sensor for coking risk tendency monitoring at the fractionating tower bottom, which faces hurdles due to intertwined spatiotemporal pattern complexities and DL model opacity. This study proposes a hybrid DL framework for soft sensor development to enhance system safety and responsiveness. The framework, applied to China's refinery with a capacity of 2.80×10^6 t/a, models the decant oil solid content soft sensor and employs the five-level risk identification, improving coking risk management at the fractionating tower bottom. The structure of this paper is as follows: Section 2 introduces the proposed framework, Section 3 details a case study for a 2.80×10^6 t/a FCCU, and Section 4 provides a summary of the findings.

2. Methodology

2.1. Problem statement

Soft sensors are crucial for process control and performance monitoring, as they estimate critical quality variables that are difficult or costly to measure in real time, thereby enhancing product quality and risk management. By integrating into feedback control systems, soft sensors provide accurate, real-time estimations, replacing expensive hardware sensors and enabling informed adjustments by human operators to maintain process stability and safety, as shown in Fig. 1.

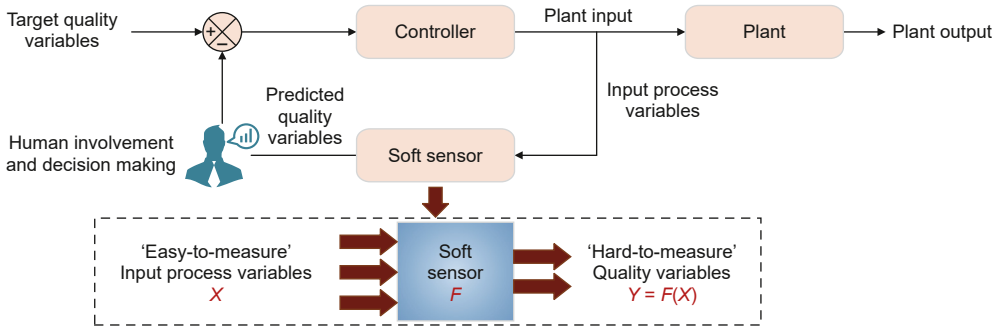

Fig. 1. The overall diagram of industrial soft sensor.

The decant oil circulation system in FCCUs plays a crucial role in process stability but is highly susceptible to coking. At the fractionating tower bottom, decant oil, containing asphaltenes, resins, and macromolecular hydrocarbons, undergoes dehydrogenation and condensation reactions at high temperatures, accelerating coke formation. Solid content increases due to catalyst loss in the reactor-regenerator system and coke deposition within the tower and circulation system. Catalyst fines, with low mechanical strength and poor sphericity, are carried into the decant oil, creating additional coking centers. These catalyst particles act as nucleation sites, adsorbing polycyclic aromatic hydrocarbons and other large organic molecules, which aggregate into coke-like structures (Oloruntoba et al., 2022; Zhang et al., 2021). Over time, the aggregation and deteriorating phase solubility lead to the transition from soft to hard coke, exacerbating fouling and operational challenges, as shown in Fig. 2. Thus, any increase in decant oil solid content—whether from catalyst or coke particles—signals heightened coking risk tendency. Since decant oil solid content is critical for monitoring catalyst loss and coking risk tendency, traditionally assessed via labor-intensive, lagging sampling and laboratory tests, developing a soft sensor for real-time measurement is imperative for enhancing operational stability, preventing downtime, and improving economic efficiency.

2.2. Overview of the proposed framework

To construct the decant oil solid content soft sensor for monitoring coking risk tendency at the fractionating tower bottom, DL, SHAP analysis, expert knowledge, and data decomposition techniques are integrated. The overarching soft sensor modeling framework is depicted in Fig. 3.

The decant oil solid content soft sensor development framework is structured into three hierarchical stages:

Feature Dataset Construction: Data preprocessing is followed by feature selection using the Filter-Wrapper method, creating the optimal feature subset to balance information content and computational efficiency.

Soft Sensor Model Construction: The 2D Convolutional Neural Network (2DCNN)-Bidirectional Gated Recurrent Unit (BiGRU)-AM architecture integrates multi-level feature extraction and bidirectional modeling to adaptively extract the spatiotemporal pattern in the FCCU's nonstationary data. Hyperparameters are optimized using the Random Search method, enhancing the generalizability of the decant oil solid content soft sensor.

Risk Identification: SHAP analysis bridges the soft sensor and risk identification by quantifying feature impacts and integrating data insights with expert knowledge to identify coking risk factors and classify risk levels. CEEMDAN decomposes signals into Intrinsic Mode Functions (IMFs), capturing time-frequency domain and fluctuations, which enhances 2DCNN's ability to identify anomalies and extract features across spatiotemporal scales.

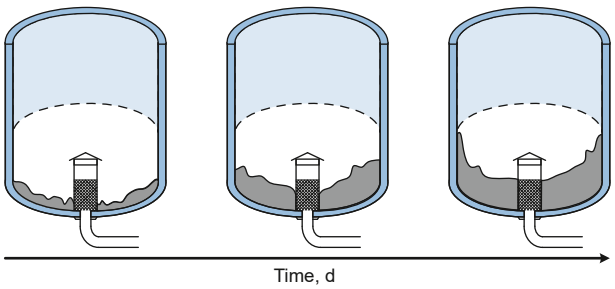

Fig. 2. The coking process at the fractionating tower bottom.

2.2.1. Filter-Wrapper method

The proposed Filter-Wrapper feature selection framework, illustrated in Fig. 4, combines the ReliefF-based Filter method with the Genetic Algorithm (GA)-based Wrapper method that utilizes K-Nearest Neighbors (KNN) for learning.

ReliefF evaluates the importance of each feature X_i by estimating its relevance to the target variable Y. The number of features and information content is balanced through the reconstructed feature contribution and cumulative feature contribution to get the rough feature dataset (Liu et al., 2022). The weight W_i for each feature is calculated using:

$$W_i = \mathrm{W}_i + \frac{\sum_{j=1}^{m}(\Delta(X_i, \mathrm{nearestHit}(j)) - \Delta(X_i, \mathrm{nearestMiss}(j)))}{m} \quad (1)$$

where m is the number of instances, Δ is a distance function, nearestHit(j) is the closest instance of the same class, and nearestMiss(j) is the closest instance of a different class.

A population of feature subsets is initialized, each subset S_k representing a potential solution. In the Wrapper stage, the performance of each subset is evaluated using a fitness function $F(S_k)$. KNN is employed to learn from the data:

$$F(S_k) = \frac{1}{n}\sum_{i=1}^{n}(y_i - \hat{y}_i)^2 \quad (2)$$

where n is the number of instances, y_i is the actual value, and $\hat{y}_i$ is the predicted value using KNN.

This integration enhances the generalization of the decant oil solid content soft sensor and reduces overfitting. The proposed Filter-Wrapper method is provided in Table S1 of the supplementary material.

2.2.2. Architecture construction for soft sensor

This architecture integrates spatial and temporal feature extraction with AM and dropout regularization for precise prediction of decant oil solid content, as detailed in Fig. 5. The process begins with an input sequence $\mathbf{X} = [X_1, X_2, \cdots, X_T]$, where each X_T is a data vector at time step T.

Initially, the 2DCNN layer processes the input $\mathbf{X}$ to capture spatial dependencies through convolutional operations. This layer produces spatial features P_T using the convolutional filter W_{conv} and bias b_{conv}, followed by the Max pooling operation to distill essential patterns and reduce computational complexity:

$$P_T = \mathrm{Pooling}(\sigma(W_{\mathrm{conv}} * X_T + b_{\mathrm{conv}})) \quad (3)$$

where σ denotes the activation function, and * represents the convolution operation. The Max pooling operation aggregates feature information, enhancing robustness by retaining critical patterns while mitigating noise.

Subsequently, the output from the 2DCNN, P_T, is then fed into a BiGRU network which captures temporal dependencies in both forward and backward directions. This results in forward hidden states $\overrightarrow{H}_T$ and backward hidden states $\overleftarrow{H}_T$:

$$\overrightarrow{H}_T = \mathrm{GRU_f}\left(P_T, \overrightarrow{H}_{T-1}\right) \quad \overleftarrow{H}_T = \mathrm{GRU_b}\left(P_T, \overleftarrow{H}_{T+1}\right) \quad (4)$$

These hidden states encapsulate the temporal evolution of spatial features, allowing the model to discern temporal patterns crucial for prediction accuracy. To mitigate overfitting and bolster generalization, the hidden states from the BiGRU layer are subjected to a Dropout layer. Dropout randomly zeroes a fraction of

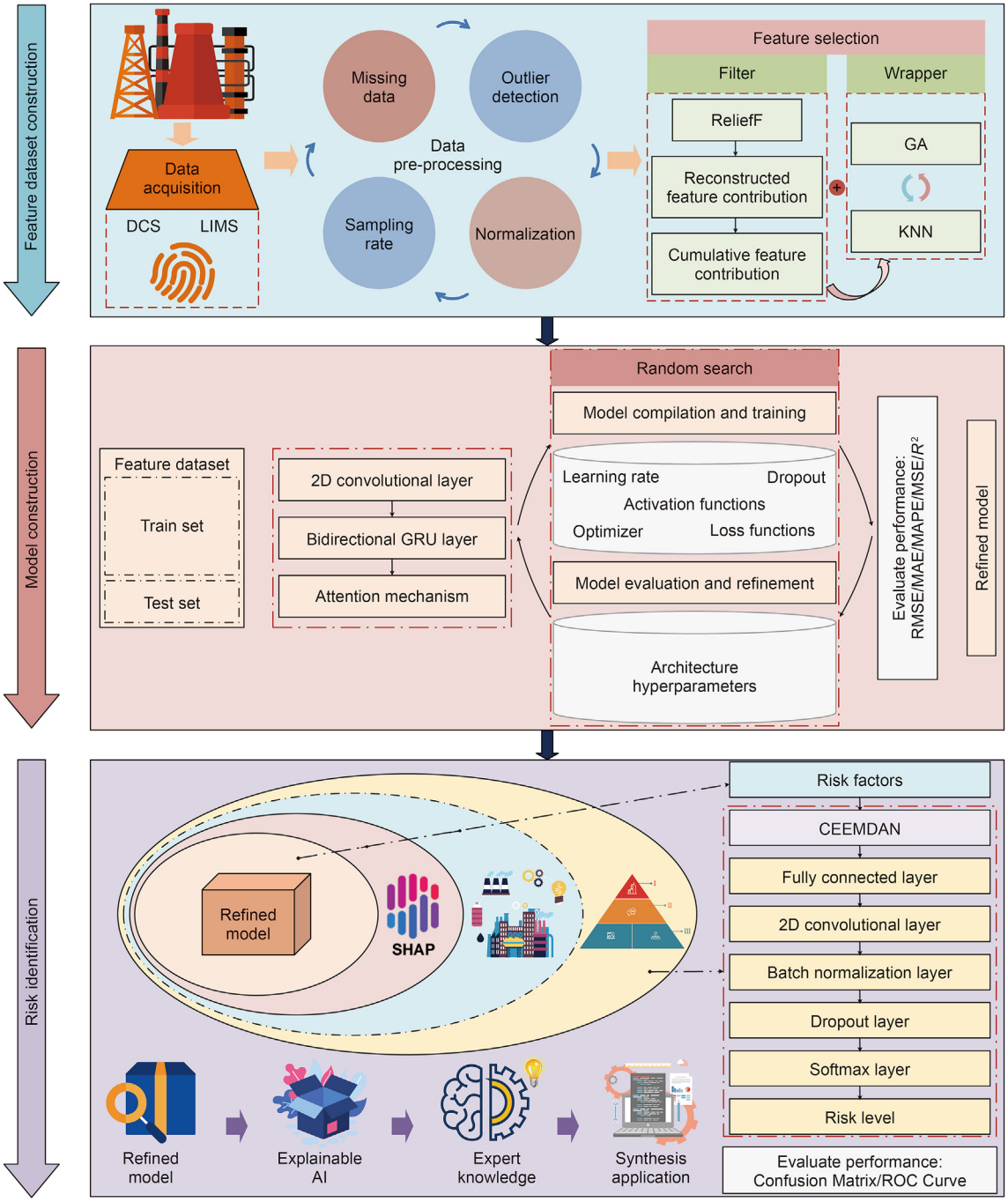

Fig. 3. The overall diagram of soft sensor development framework.

input units during training, as controlled by the dropout rate p, thereby promoting redundant representations:

$$H_T^{\text{Drop}} = \text{Dropout}(H_T, p) \tag{5}$$

where H_T^{Drop} represents the BiGRU hidden states post-dropout. This mechanism enhances model robustness by preventing excessive reliance on specific feature subsets.

The dropout-processed hidden states H_T^{Drop} are then refined using an AM, which assigns weights to each time step to create a context vector C_T, emphasizing the most pertinent features for prediction. The attention scores α_T are computed through a softmax function on similarity scores v_T:

$$v_T = \tanh\left(W_\alpha H_T^{\text{Drop}} + b_\alpha\right) \tag{6}$$

$$\alpha_T = \frac{\exp(v_T)}{\sum_{T'} \exp(v_{T'})} \tag{7}$$

$$C_T = \sum_{i=1}^{T} \alpha_T H_T^{\text{Drop}} \tag{8}$$

where W_α and b_α are the parameters of the attention layer. The AM selectively enhances significant spatiotemporal features, aligning model focus with critical sequence aspects.

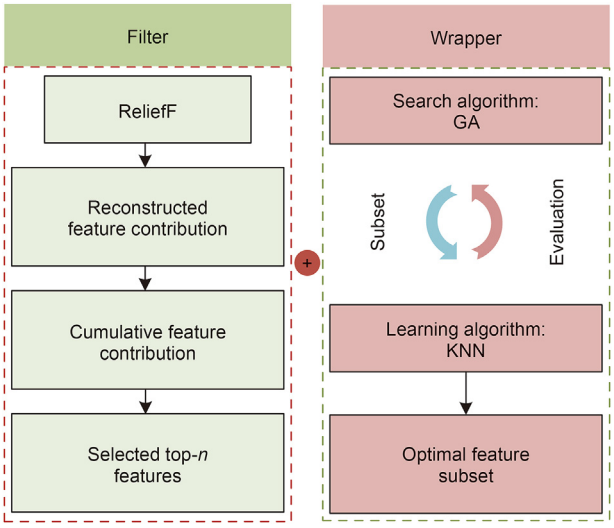

Fig. 4. The proposed Filter-Wrapper feature selection schematic diagram.

Finally, the context vector C_T, enriched with both spatial and temporal features, is passed through a dense layer to generate the final prediction $\hat{Y}_T$:

$$\hat{Y}_T = \sigma(W_d C_T + b_d) \tag{9}$$

where W_d represents the weights, b_d the biases, and σ the activation function used to produce the output. The dense layer integrates the learned features to output a prediction that reflects the current state of decant oil solid content.

The 2DCNN architecture effectively enhances model accuracy in industrial applications by capturing spatial correlations among operational parameters (Yuan et al., 2020). Its hierarchical feature extraction through convolution layers enables fine-grained and broader spatial pattern recognition, as depicted in Fig. 6, essential for robust coking risk tendency monitoring in FCCU, while parameter sharing and translation invariance improve model performance.

The 2DCNN operator can be expressed as Eq. (10).

$$v_{ij}^{xy} = f\left(\sum_z \sum_{m=0}^{M_i-1} \sum_{n=0}^{N_i-1} \omega_{ijk}^{mn} v_{(i-1)k}^{(x+m)(y+n)} + b_{ij}\right) \tag{10}$$

where v_{ij}^{xy} is the value of the cell at the spatial location (x, y) in the jth element map of the ith layer, $f(\cdot)$ is the activation function, k is the index of the set of feature maps connected to the $(i-1)$th layer of the current feature map, ω_{ijk}^{mn} denotes the value at the ijk position (m, n) of the kernel connected to the kth feature map, M_i and N_i denote the height and width of the kernel, and b_{ij} denotes the deviation of this feature map.

In Fig. 7, the architecture employs AM for its superior capability in selective feature aggregation and contextual awareness, dynamically assigning importance to features at each time step. Unlike fully connected layers that treat all features uniformly, AM adjusts weights contextually, capturing intricate spatiotemporal dependencies crucial for accurate risk monitoring in FCCU. GRU, a simpler variant of LSTM with fewer parameters, uses update and reset gates for improved convergence and information retention. Traditional sequential models like LSTM and GRU have limitations in capturing relationships between distant data points. To overcome this, the BiGRU is employed, processing input time series through forward and backward GRU units explained by the following Eqs. (11)–(13), enhancing the ability to learn features from both directions and improving long-period time dependence modeling. This dynamic, responsive feature aggregation and bidirectional processing enhance model performance.

$$\overrightarrow{H}_t = \mathrm{GRU}\left(x_t \cdot \overrightarrow{H}_{t-1}\right) \tag{11}$$

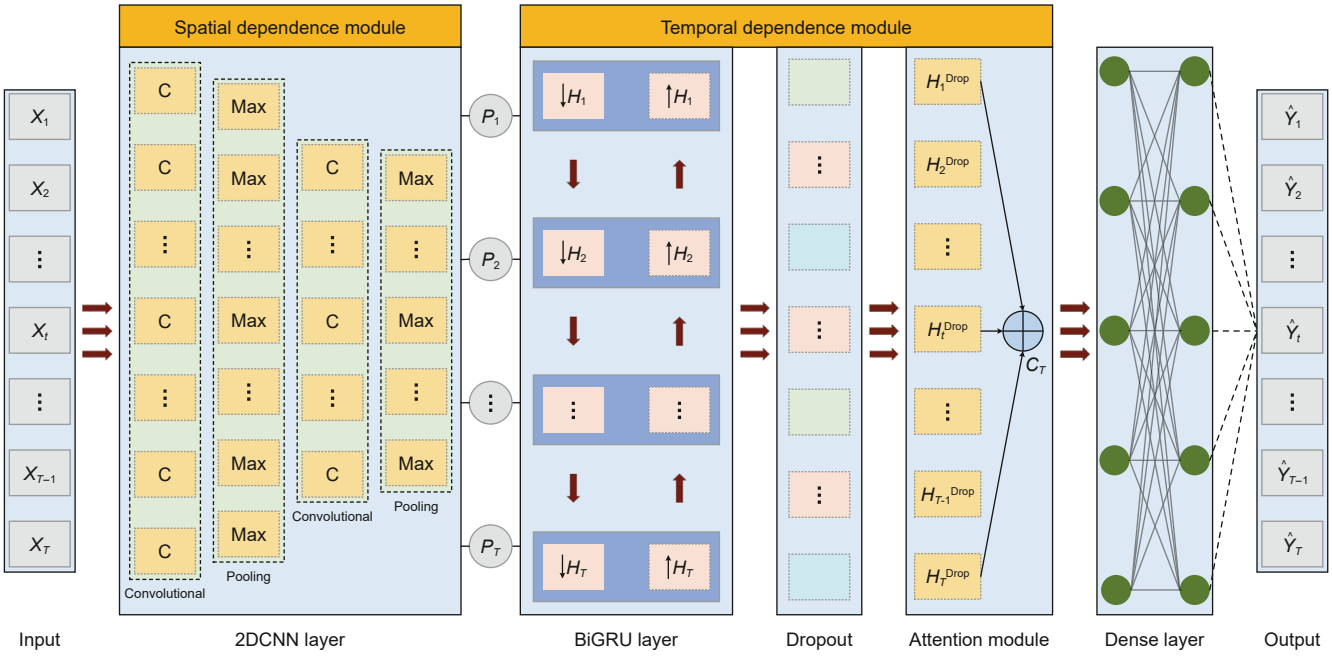

Fig. 5. The architecture of coking soft sensor.

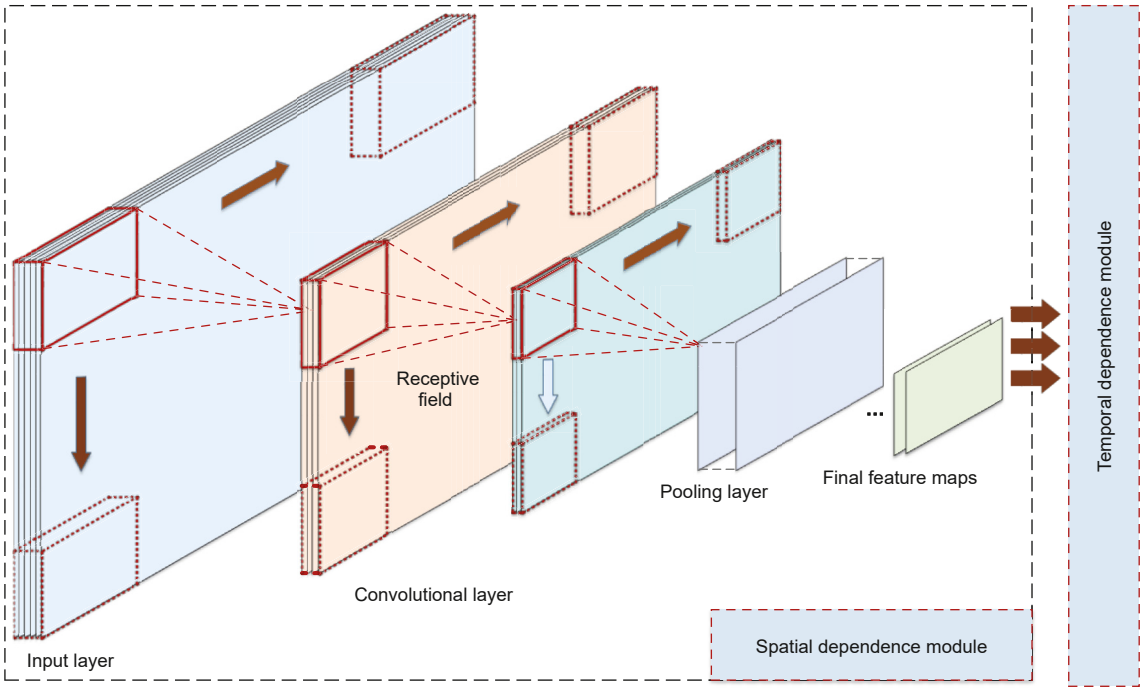

Fig. 6. The architecture of spatial dependence module based 2DCNN.

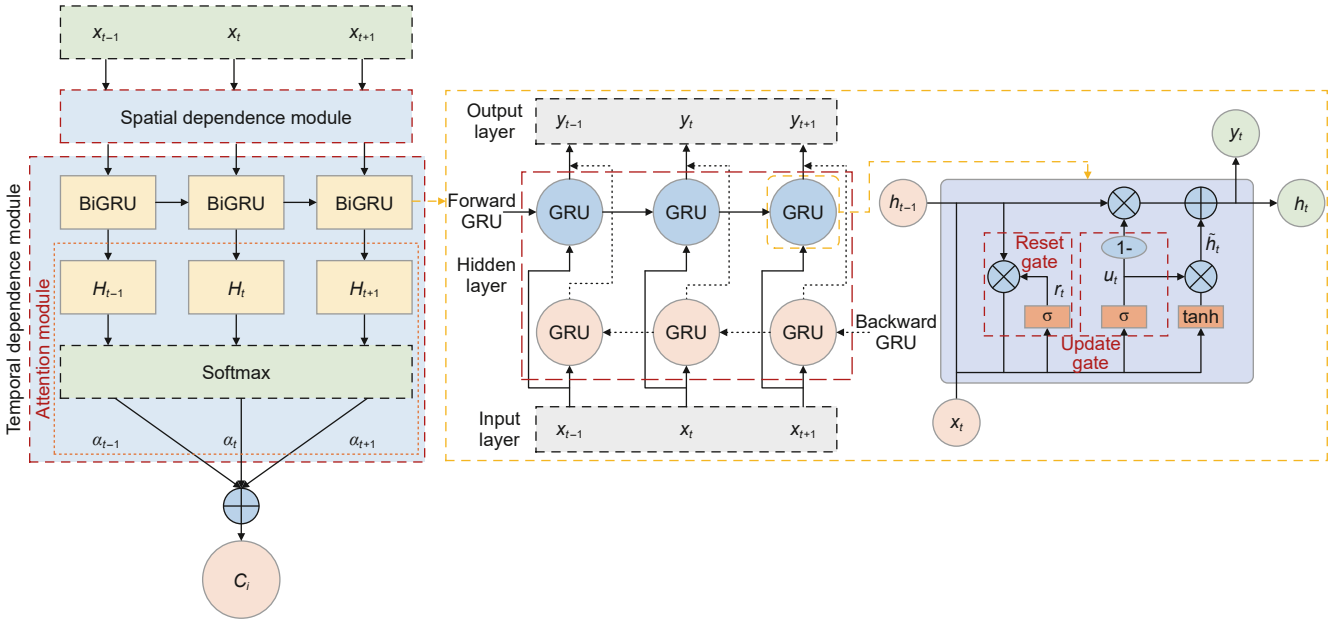

Fig. 7. The architecture of temporal dependence module based BiGRU.

$$\overleftarrow{H}_t = \mathrm{GRU}\left(x_t \cdot \overleftarrow{H}_{t+1}\right) \tag{12}$$

$$H_t = w_t \overrightarrow{H}_t + v_t \overleftarrow{H}_t + b_H \tag{13}$$

where GRU(•) denotes the nonlinear transformation. The weights w_t and v_t correspond to the forward hidden state $\overrightarrow{H}_{t-1}$ and reverse hidden state $\overleftarrow{H}_{t+1}$ for BiGRU, respectively. The term b_H represents to bias associated with the hidden state at t time.

2.2.3. Methodology for risk identification

Fig. 8 illustrates the framework for coking risk identification. Initially, CEEMDAN decomposes the signals into multiple IMFs and reduces noise handling complex nonlinear and non-stationary signals. The 2DCNN then extracts intricate spatiotemporal patterns from the IMFs while capturing local dependencies and interactions crucial for adapting to different operational conditions. SHAP analysis quantifies the contributions of features to decant oil solid content prediction. This interpretable layer is refined through expert knowledge, validating key operational factors like temperature, flow, and pressure. This hybrid approach enhances model

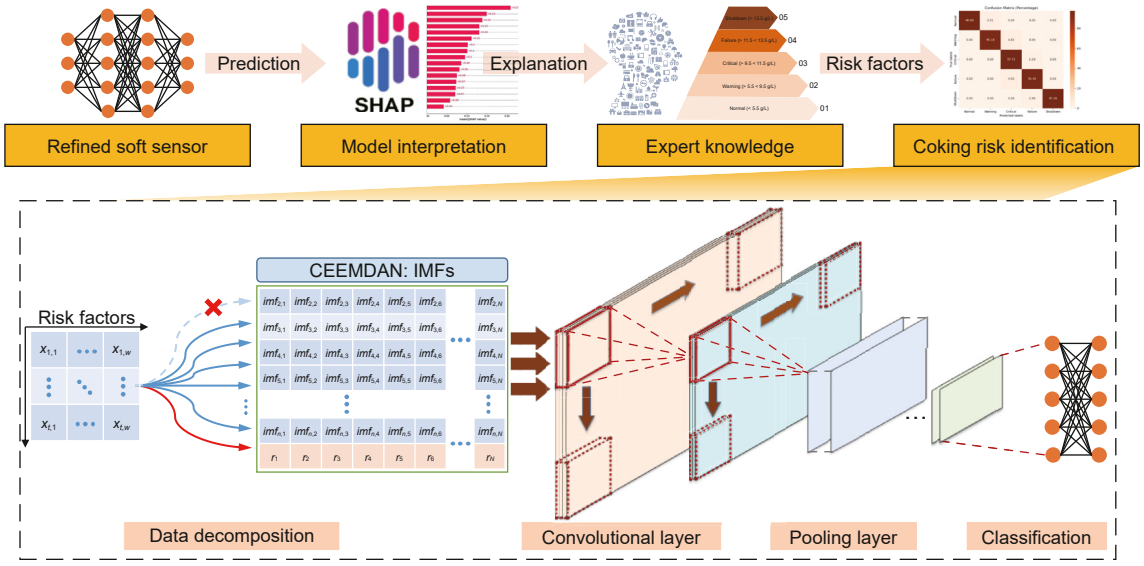

Fig. 8. The diagram of coking risk identification.

transparency, credibility, and precise, real-time risk assessment, advancing predictive maintenance in monitoring coking risk tendency at the fractionating tower bottom.

Despite the absence of the consensus in the industry or literature for the boundary values and corresponding risk levels of decant oil solid content—largely attributable to process variability across refineries and the consequent reliance on individual operational experience—this study adopts expert experience, recognized as the reliable approach to risk ranking, by drawing on extensive plant knowledge and operator insights to define the boundary values for decant oil solid content. Since catalyst fines, coke particles, and other impurities collectively constitute decant oil solid content, with catalyst fines predominating and accelerating solid accumulation and promoting coke formation, these thresholds are essential for preserving operational stability. By the refinery's operational guidelines and empirical observations of how solid content fluctuations affect equipment performance, 5.5 and 13.5 g/L are designated as lower and upper limits, corresponding to normal and shutdown conditions, respectively, while intermediate intervals delineate warning, serious, and failure risk levels. Notably, the wider interval (5.5–9.5 g/L) enables early detection and flexible intervention, thus minimizing unnecessary adjustments, whereas the narrower intervals (9.5–11.5 g/L and 11.5–13.5 g/L) provide more precise control under higher risk scenarios, as shown in Fig. 9. This five-level risk classification approach provides structured monitoring, targeted safety responses, enhanced operational stability, and an optimal balance of cost with risk, facilitating long-term stable operation.

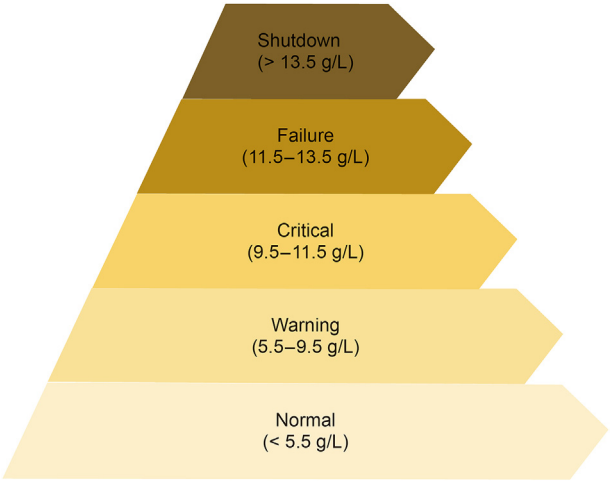

Fig. 9. The decant oil solid content risk levels.

Model interpretability involves the understanding intrinsic decision-making mechanism within the prediction. SHAP, grounded in game theory, allocates optimal credits using Shapley values to estimate feature importance. It provides clear visualizations and ensures fair distribution of prediction credits, enhancing trust in the model. The following is a brief description of its principle.

$$\phi(i)=\sum_{S\subset\{x^1,\ldots,x^p\}/\{x^j\}}\frac{|S|!(p-|S|-1)!}{p!}\left(f(S\bigcup\{x^p\})-f(S)\right) \tag{14}$$

where $\phi(i)$ denotes the attribute value for each feature i, $f(\cdot)$ is the soft sensor's output, S represents the subset of risk factors, x^j represents the feature j of risk factors, p is the number of risk factors.

Decoupling the multiscale information from highly nonlinear FCC industrial data, which encompasses process details such as flow, reaction, mass transfer, and heat transfer, is crucial for accurately identifying coking risks. The advantage of the CEEMDAN-2DCNN architecture in FCCU risk identification lies in its ability to effectively decompose noise and nonlinear interferences while capturing spatiotemporal dependencies. CEEMDAN decomposes risk factors into IMFs, effectively extracting multiscale information and reducing noise interference. Combined with 2DCNN's convolution operations in both temporal and spatial dimensions, this approach captures spatiotemporal dependencies among the IMFs. For $X(t)$, representing the signal of risks factors, the calculation of the latter modal component continues until all the residual signals $R(t)$ can no longer be decomposed. The termination criterion is that the maximum number of extremum points of $R(t)$ should not exceed two. When the algorithm terminates, if the number of modal components is T, the final $R(t)$ is given by Eq. (15):

$$R(t) = X(t) - \sum_{i-1}^{T} \mathrm{IMF}_i(t) \tag{15}$$

Finally, the original signal $X(t)$ is expressed as shown in Eq. (16):

$$X(t) = \sum_{i-1}^{T} \mathrm{IMF}_i(t) + R(t) \tag{16}$$

3. Case study

3.1. Descriptions of FCCU

The FCCU comprises several interconnected operational units, including the reactor-regenerator system, fractionation, and absorption stabilization, as shown in Fig. 10. These subsystems exhibit strong coupling correlations, resulting in high-dimensional, spatiotemporally correlated data. Given the continuous nature of production, fluctuations in crude oil properties and market demands lead to dynamic changes in the production environment and operational conditions. Consequently, various operating parameters require periodic adjustments, making FCCU data highly nonlinear and complex. Abnormal conditions, such as coking and catalyst loss, frequently occur, posing significant safety hazards, causing unplanned shutdowns, and reducing production efficiency. In particular, monitoring decant oil solid content is crucial for assessing the coking risk tendency at the fractionating tower and circulation system. However, current daily sampling methods are inefficient and insufficient for real-time decision-making. Therefore, developing a soft sensor for decant oil solid content is vital for enhancing FCCU operational stability, improving safety, and optimizing overall production efficiency.

3.2. Decant oil solid content soft sensor

3.2.1. Optimal feature dataset construction

The industrial data from a refinery in China, with a processing capacity of 2.80×10^6 t/a, spans from June 2018 to September 2021 and consists of DCS data with six selected variables: external heater density, dry gas outlet flow, diesel outlet flow, cold feed flow, decant oil recycle flow to the tower, and external heater air riser density, as shown in Fig. 11. DCS data, with its high sampling frequency, real-time availability, and direct correlation with operational parameters, provides the necessary temporal resolution and consistency required for accurate and reliable online monitoring. In contrast, LIMS data is characterized by low sampling frequency, significant time lag, low data density, and frequency mismatches among different physical variables, limiting its applicability for deployment in industrial field applications. The high dimensionality and non-stationarity of the data demand advanced feature selection and extraction methods to capture essential spatiotemporal patterns. Additionally, sensor errors and production adjustments introduce noise and nonlinearity, necessitating a robust and adaptable model for accurately monitoring the coking risk tendency. To ensure consistency between input and output variables, the high-frequency DCS data (one sample per minute) is downsampled to a daily frequency. This frequency adjustment aligns with the low-frequency measurement of decant oil solid content, which exhibits long-term trends with minimal short-term fluctuations, supports practical industrial decision-making, and better aligns with industrial operating conditions. Notably, a nearly two-month maintenance period from February 8 to March 21, 2020, resulted in a synchronized downward trend across multiple variables, followed by gradual recovery. This period serves as an important validation of the decant oil solid content soft sensor, demonstrating its generalizability and effectiveness in capturing dynamic process variations.

The dataset comprises 102 operational variables. Initially, the ReliefF-based Filter method is used for preliminary selection. Fig. 12(a) reveals the weight of each feature in predicting decant oil solid content, with the first 20 variables having significant and varied weights, indicating their importance. Variables 20 to 80 show comparable importance with slower weight change, while variables after 80 have smaller and less varied weights. Fig. 12(b) illustrates the cumulative contributions of feature weights. The 19, 35, and 47 variables account for cumulative contributions of 50%, 70%, and 90%, respectively. The addition of variables slows from 16 to 12 when cumulative contributions increase by 20%. However, the final 10% of cumulative contributions involve 55 variables, adding 5.5 per 1% increase, indicating lesser relevance. Thus, setting a 90% cumulative contribution threshold reduces the number of variables from 102 to 47.

Fig. 13 shows that the GA-KNN-based Wrapper method yields a progressive reduction in $F(S_k)$ and feature count with each iteration, ultimately stabilizing at 17 variables and achieving a Mean Absolute Percentage Error (MAPE) of 6.3%. The optimal feature dataset and associated descriptions for the decant oil solid content soft sensor is detailed in Table S2 of the supplementary material.

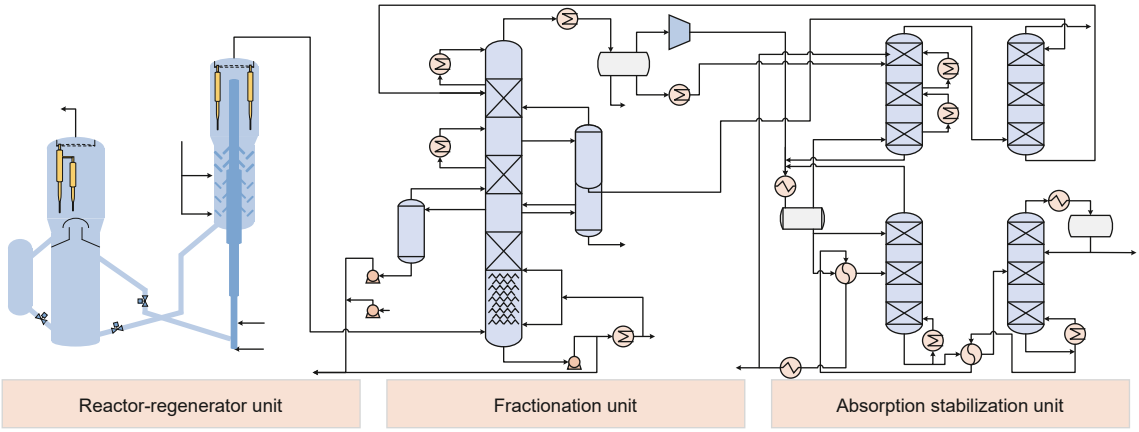

Fig. 10. The flowchart of FCCU.

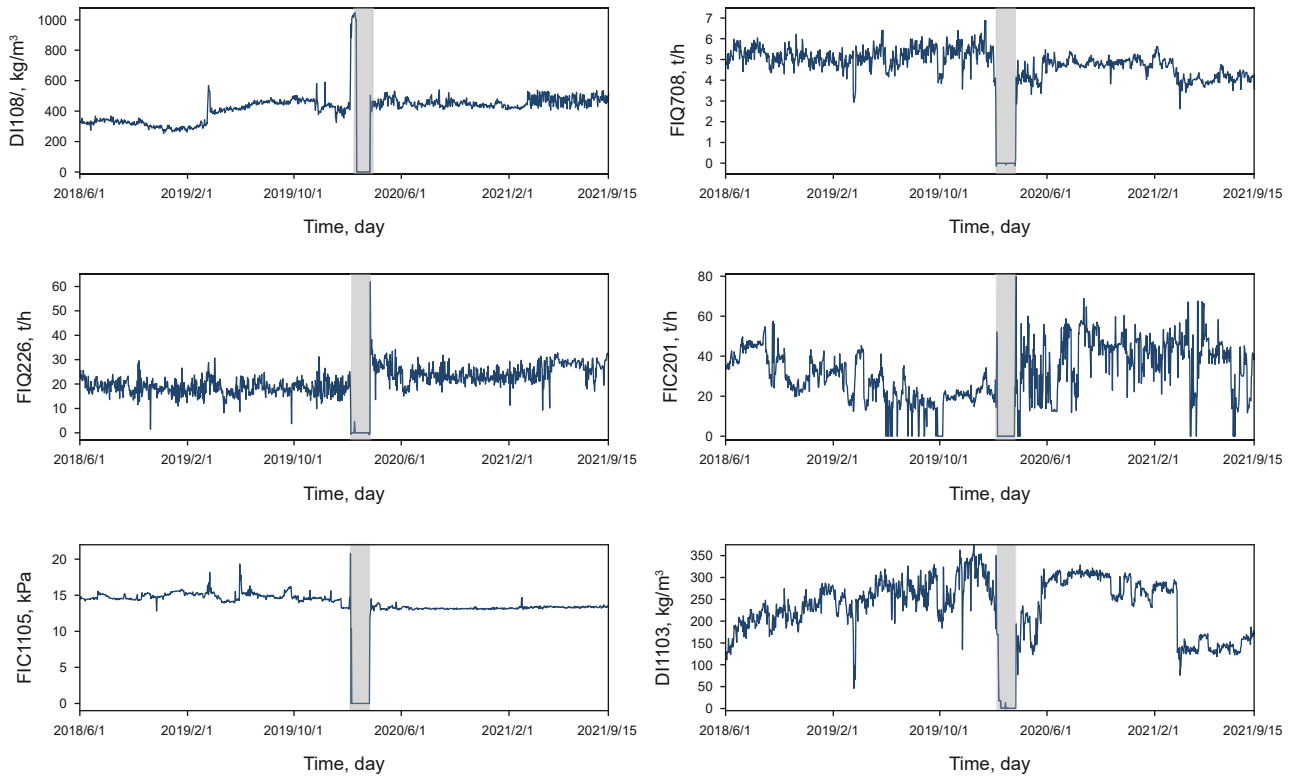

Fig. 11. The typical DCS data presentation for FCCU.

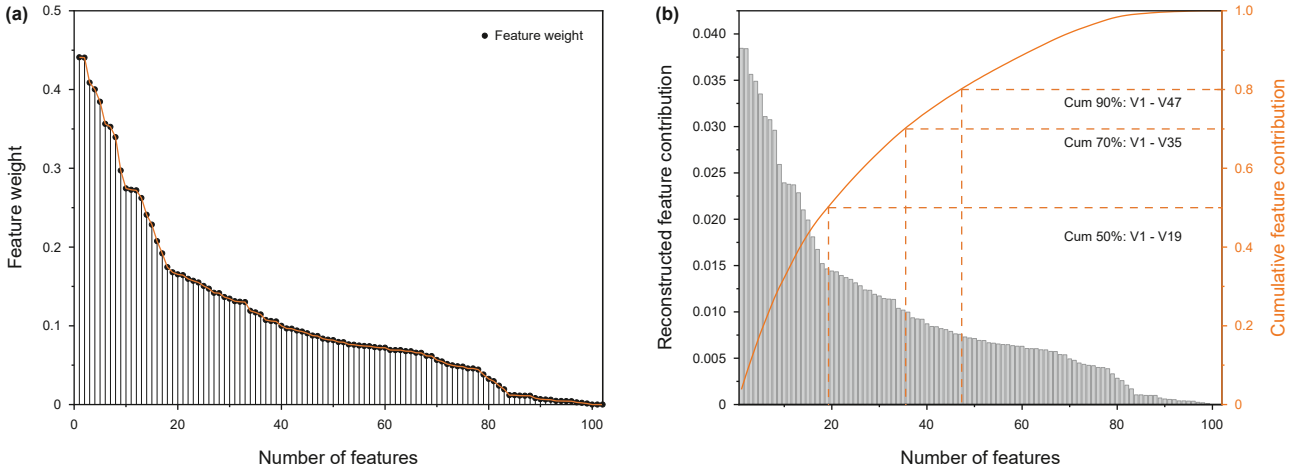

Fig. 12. **(a)** Results of feature weights, **(b)** reconstruction and cumulative feature contribution.

3.2.2. *Hyperparameter optimization*

Constructing a robust decant oil solid content soft sensor in real industrial settings demands detailed consideration of architecture design and hyperparameter optimization, balancing factors such as model complexity, computational efficiency, and performance. The running environment is on an Intel(R) Core(TM) i9-10980XE CPU @ 3.00 GHz, 64.0 GB of RAM, and Windows 10. The decant oil solid content soft sensor uses the keras_tuner package to conduct RandomSearch optimization, allowing for exploration of the hyperparameter space, integrated with TensorFlow 2.x and Keras, thus enabling the discovery of the optimal configuration for enhanced model performance and generalization. Table 1 presents the hyperparameters to be optimized, including the conv1_filters, conv2_filters, conv3_filters, lstm_units, dropout_rate, and optimizer.

As shown in Fig. 14, hyperparameter optimization is crucial for balancing computational efficiency and generalization, ensuring robust performance under varying operational conditions. The optimal architecture, detailed in Table S3 of the supplementary material, employs sequential convolution layers (filters of 16, 32, and 16 with kernel sizes of 5 × 5, 4 × 4, and 3 × 3, respectively) to capture spatial patterns effectively. A 32-unit BiGRU captures temporal dynamics, leveraging bidirectional learning for the long-period dependency. Adaptive AM enhances the soft sensor's focus on the critical spatiotemporal pattern, while batch normalization and a dropout rate of 0.5 bolster stability and mitigate overfitting.

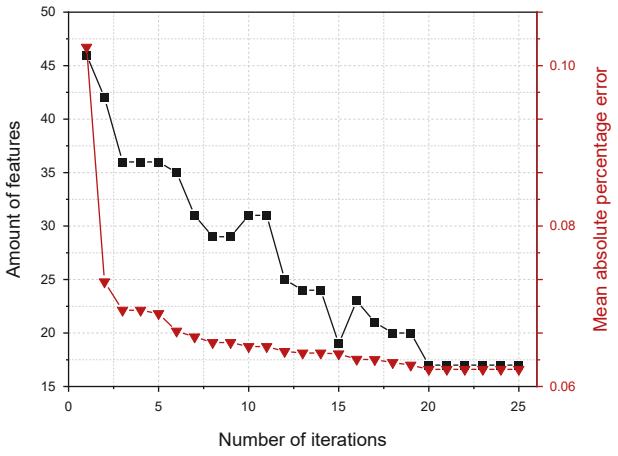

Fig. 13. Result of Wrapper process.

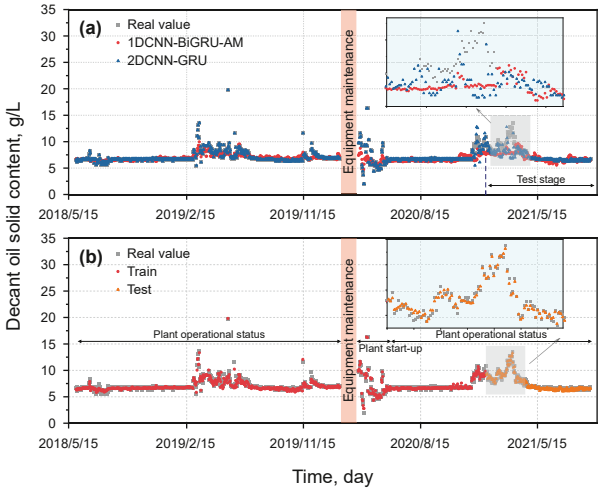

Fig. 15. **(a)** The prediction results of 1DCNN-BiGRU-AM and 2DCNN-BiGRU architectures, **(b)** the prediction result of 2DCNN-BiGRU-AM architecture.

Table 1
Configurations of the hyperparameters range.

Hyperparameters	Selection range
Conv1_filters	[16, 32, 64]
Conv2_filters	[16, 32, 64]
Conv3_filters	[16, 32, 64]
GRU_units	[32, 64, 128]
Dropout_rate	[0.2, 0.3, 0.5]
Optimizer	[Adam, Rmsprop, SGD]

Optimized with an MAE loss function, batch size of 24, and time step of 8, this configuration enables real-time decant oil solid content monitoring at the fractionating tower bottom and aids decision-making.

3.2.3. *Performance comparison analysis*

Fig. 15 shows the comparison prediction results. To evaluate the performance of the spatial and temporal pattern extraction modules, the ablative study is constructed to compare the spatial dependency extraction of 2DCNN versus 1DCNN and the long-term temporal extraction capabilities of BiGRU-AM versus GRU. The 1DCNN-BiGRU-AM and 2DCNN-BiGRU architectural parameters are shown in Tables S4–S5 of the supplementary material.

During the maintenance period from 8 February to March 21, 2020, data gaps are intentionally left unfilled to evaluate model generalization and robustness. The 1DCNN-BiGRU-AM architecture struggles with high-frequency variations (see Fig. 15(a)), while the 2DCNN-GRU architecture shows performance deterioration post-maintenance. In high-dimensional industrial data with spatial correlations, 2DCNN outperformed 1DCNN in capturing spatial dependencies, effectively modeling interactions between operational variables in the reactor-regenerator and fractionating system. Interdependent factors, such as fractionation tower bottom level, temperature, decant oil circulation volume, and recycled volume, all impact decant oil solid content. By extracting these spatial dependencies, 2DCNN enhances predictive accuracy under complex operational conditions.

BiGRU-AM further strengthens the architecture by capturing the long-term dependence and emphasizing crucial temporal patterns through AM, which improves recognition of trends and significant temporal signals, including temperature and pressure fluctuations that may indicate the coking risk tendency. This ability to identify essential patterns forms a foundation for reliable risk monitoring, facilitating early warning and informed decision-making. The 2DCNN-BiGRU-AM architecture thus demonstrates adaptability to fluctuations due to maintenance and operational adjustments, accommodating new data distributions while maintaining predictive accuracy (see Fig. 15(b)). Combining 2DCNN for spatial feature extraction with BiGRU-AM's temporal modeling, this architecture proves practical for FCCU applications, characterized by complex reactions, dynamic production schedules, interconnected subsystems, and non-stationary data.

As shown in Fig. 16(a), the 2DCNN-BiGRU-AM architecture excels across multiple error indicators, including MSE, Root Mean

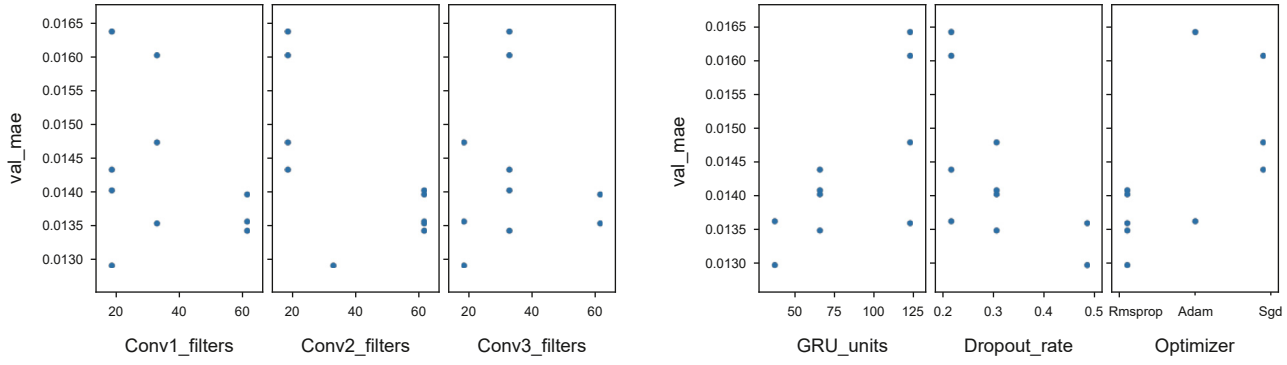

Fig. 14. The results of hyperparameters tuning.

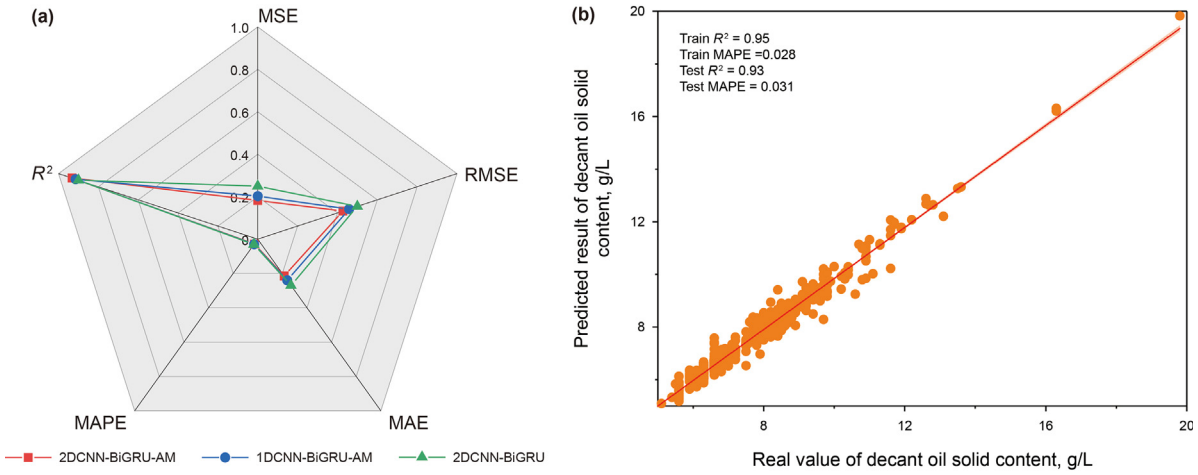

Fig. 16. **(a)** Error analysis of five indicators, **(b)** fitted curves plot of predicted vs. actual values.

Table 2
Comparison results of computational time, memory usage, and total parameters.

Model	Training time, s	Testing time, s	Memory, MB	Total parameters
1DCNN-BiGRU-AM	240.5	0.9232	2.111	19460
2DCNN-GRU	249.7	0.8558	2.025	26321
2DCNN-BiGRU-AM	299.3	0.9288	2.168	30788

Squared Error (RMSE), MAE, and MAPE. The decant oil solid content soft sensor (Fig. 16(b)) achieves R^2 values of 0.95 and 0.93 with MAPE values of 0.028 and 0.031 on the training and test sets. This high predictive accuracy, combined with its robustness and adaptability to dynamic data, underscores the architecture's significant advantages for monitoring coking tendency at the fractionating tower bottom.

Next, the decant oil solid content soft sensor is compared with the above comparison architectures regarding computational time, memory usage, and the number of parameters on the FCCU dataset, as shown in Table 2. The comparison results highlight the 2DCNN-BiGRU-AM architecture's capability for decant oil solid content monitoring without requiring more computational resources.

3.3. Coking risk identification

Fig. 17(a) shows the impact of individual feature variables of the decant oil solid content soft sensor. SHAP values quantify each

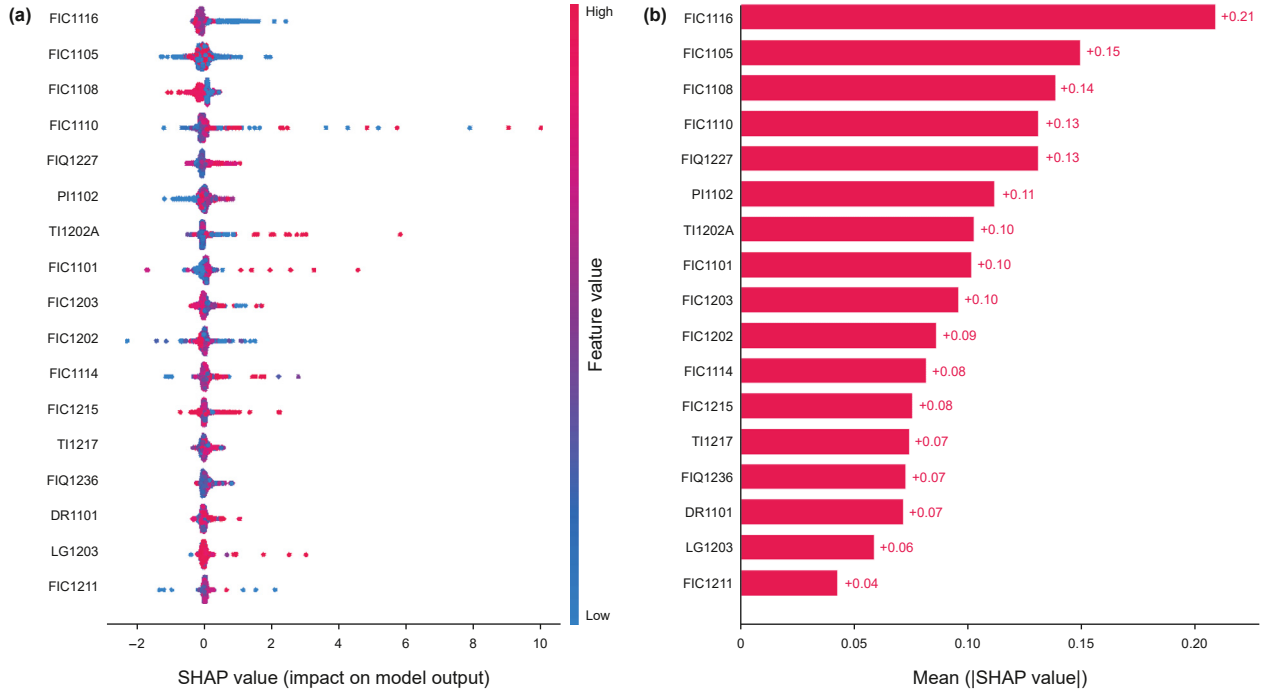

Fig. 17. **(a)** Impact of feature variables on model output using SHAP values, **(b)** the average SHAP values of feature variables.

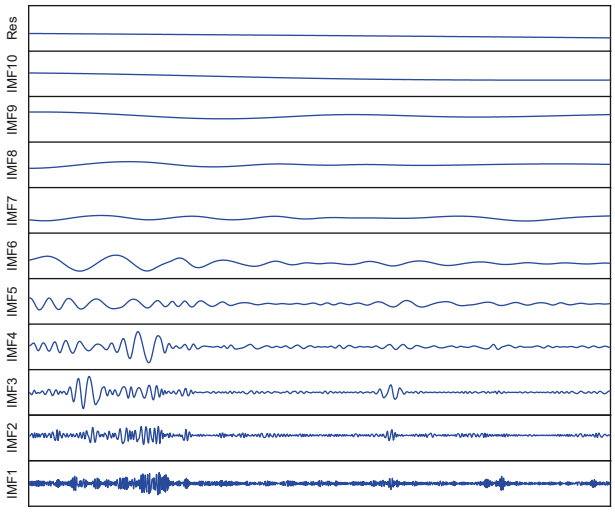

Fig. 18. The results of TI1202A by CEEMDAN decomposition.

variable's positive or negative contribution to the output, while the dot distribution reflects the influence of variable values. The color gradient (blue for lower values, red for higher values) illustrates the relationship between feature variables and decant oil solid content. Fig. 17(b) displays the average SHAP values, highlighting each variable's overall contribution to predictions. In FCCU operations, FIC1116 regulates fluidized air in the external heat exchanger, crucial for dissipating excess heat from the regenerator and maintaining thermal equilibrium. Effective control of the regenerator's heat load is vital for stable operation. FIC1105 manages the two-phase fluidized air flow rate, which is critical for catalyst circulation between units. Furthermore, TI1202A and PI1102, which control the temperature and feed pressure of raw oil to R-101A, play a key role in stabilizing the reaction-regeneration system, affecting the mixing, vaporization, and reaction of crude oil with the regenerated catalyst.

CEEMDAN is an effective tool for addressing the time-varying and nonstationary characteristics of the four risk factors identified through SHAP analysis. As illustrated in Fig. 18, CEEMDAN decomposes TI1202A into individual IMFs, isolating the time-frequency domain and reducing noise. This decomposition yields multiscale features that significantly enhance the generalization capabilities of the 2DCNN across various operational conditions, improving its ability to detect early-stage risks.

Table S6 in the supplementary material provides the detailed parameters of the risk identification architecture, which classifies decant oil solid content into five risk levels by integrating CEEMDAN-based decomposition with 2DCNN. The confusion matrix in Fig. 19(a) illustrates precise classification across "Normal," "Warning," "Critical," "Failure," and "Shutdown" states, with minor misclassifications occurring mainly between adjacent levels during transitional phases, likely due to dynamic shifts in operational conditions and response delays. Achieving an average accuracy of 96.42%, the architecture effectively detects subtle changes, demonstrating robustness under complex conditions, such as maintenance and operational adjustments. As shown in Fig. 19(b), the accuracy, precision, recall, and F1 scores are 0.961, 0.986, 0.972, and 0.983, underscoring its strong signal-processing capabilities and adaptability to complex operational conditions, validating its reliability in decant oil solid content monitoring.

The ROC curve in Fig. 20 illustrates the model's classification performance across risk levels, plotting the true positive rate (TPR) against the false positive rate (FPR). Notably, the ROC curve is unaffected by the risk level distribution, with an AUC value closer to 1 indicating stronger discrimination capability for decant oil solid content risk levels. Achieving a mean AUC of 0.964, the model

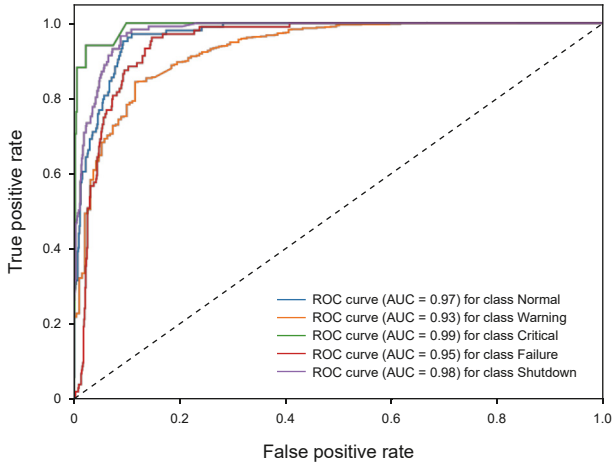

Fig. 20. The ROC curve of risk identification.

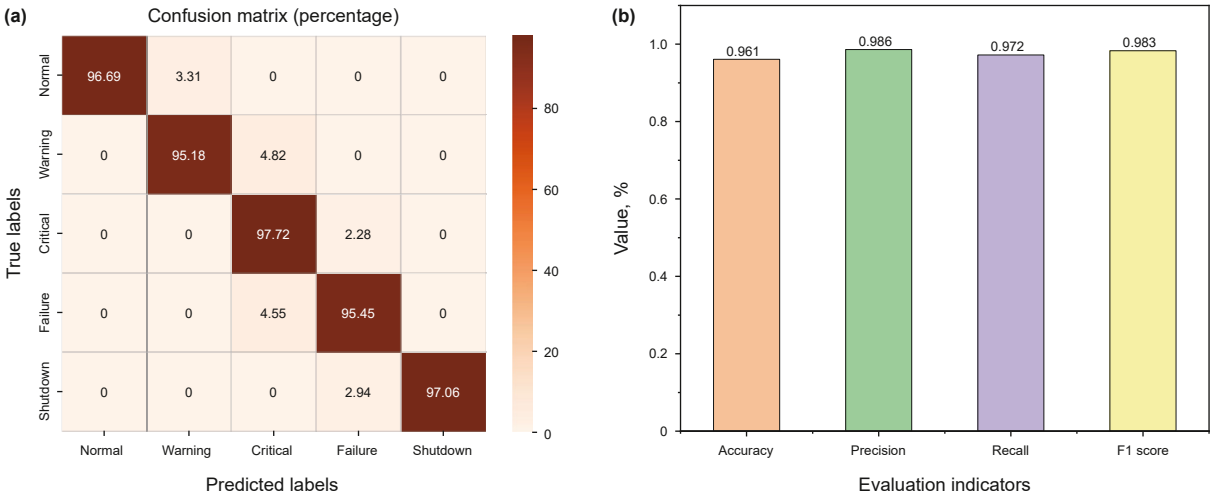

Fig. 19. **(a)** The confusion matrix for risk identification, **(b)** the evaluation indicators for risk identification.

demonstrates excellent classification results, underscoring the soft sensor's effectiveness in distinguishing between risk states in fractionating tower bottom scenarios. An analysis of Fig. 19(a) alongside the ROC curve reveals variability in recognizing specific risk states: the model accurately identifies "Critical" and "Shutdown" states, with accuracies of 97.72% and 97.06%, likely due to the distinctive features of these states. "Normal" state recognition also performs well, with an accuracy of 96.69%, highlighting robust detection under stable conditions. However, effectiveness decreases for the "Warning" and "Failure" states, particularly in transitional phases like risk onset or rapid changes, as indicated by misclassification rates of 4.82% and 4.55%, respectively. Despite challenges in managing boundary uncertainties, the risk identification architecture demonstrates strong overall precision and adaptability across risk levels.

4. Conclusion

This paper presents a framework for developing decant oil solid content soft sensor that integrates DL, interpretable analytics, expert knowledge, and data decomposition techniques. Implemented in a Chinese refinery with a processing capacity of 2.80×10^6 t/a, this framework facilitates coking risk management at the fractionating tower bottom, enabling proactive staff intervention and ensuring stable production. The following conclusions are drawn:

- By applying the ReliefF-based Filter method followed by the GA-KNN-based Wrapper method to 102 operational variables, 19, 35, and 47 variables are selected, contributing 50%, 70%, and 90% of cumulative importance. Ultimately, this process reduces the variables to 17, resulting in a stable MAPE of 6.3% for the decant oil solid content soft sensor.
- The 2DCNN-BiGRU-AM architecture effectively captures spatial and temporal dependencies in nonstationary data, achieving an R^2 of 0.93 on the test dataset for the decant oil solid content soft sensor, post-optimization of the hyperparameters, without a significant increase in computational resource consumption.
- The SHAP methodology, combined with expert knowledge, identifies FIC1116, FIC1105, TI1202A, and PI1102 as key risk factors involving temperature, flow, and pressure variables. By integrating CEEMDAN's multiscale decomposition with 2DCNN's spatiotemporal feature extraction, the architecture attains the accuracy of 96.42%, demonstrating robust and precise five-level risk identification.

The proposed approach improves risk management and predictive maintenance. Future work will focus on integrating high-frequency DCS data with lower-frequency LIMS data for more accurate real-time industrial risk monitoring. Additionally, addressing scalability and robustness challenges through advanced AI techniques and cloud-edge-device architectures will enhance computational efficiency.

CRediT authorship contribution statement

Nan Liu: Writing – review & editing, Writing – original draft, Methodology, Data curation, Conceptualization. **Chun-Meng Zhu:** Validation, Investigation. **Yu-Hui Li:** Investigation. **Yun-Peng Zhao:** Supervision. **Xiao-Gang Shi:** Supervision. **Xing-Ying Lan:** Supervision, Funding acquisition.

Declaration of competing interest

The authors declared that they have no conflicts of interest to this work.We declare that we have no financial and personal relationships with other people or organizations that can inappropriately influence our work, there is no professional or other personal interest of any nature or kind in any product, service and/or company that could be construed as influencing the position presented in, or the review of, the manuscript entitled.

Acknowledgements

The present work is financially supported by the Innovative Research Group Project of the National Natural Science Foundation of China (22021004), and Sinopec Major Science and Technology Projects (321123-1), and hereby their supports are sincerely acknowledged.

Appendix A. Supplementary data

Supplementary data to this article can be found online at https://doi.org/10.1016/j.petsci.2025.04.006.

References

Agarwal, P., Aghaee, M., Tamer, M., Budman, H., 2022. A novel unsupervised approach for batch process monitoring using deep learning. Comput. Chem. Eng. 159, 107694. https://doi.org/10.1016/j.compchemeng.2022.107694.

Arunthavanathan, R., Khan, F., Ahmed, S., Imtiaz, S., 2021. A deep learning model for process fault prognosis. Process Saf. Environ. Prot. 154, 467–479. https://doi.org/10.1016/j.psep.2021.08.022.

Bhakte, A., Pakkiriswamy, V., Srinivasan, R., 2022. An explainable artificial intelligence based approach for interpretation of fault classification results from deep neural networks. Chem. Eng. Sci. 250, 117373. https://doi.org/10.1016/j.ces.2021.117373.

Cui, Z., Sun, Y., Li, Z., Liu, B., Tian, W., 2024. Traceability analysis of wastewater in coal to ethylene glycol process based on dynamic simulation and deep learning. J. Clean. Prod. 443, 141133. https://doi.org/10.1016/j.jclepro.2024.141133.

Ferreira, J., Pedemonte, M., Torres, A.I., 2022. Development of a machine learning-based soft sensor for an oil refinery's distillation column. Comput. Chem. Eng. 161, 107756. https://doi.org/10.1016/j.compchemeng.2022.107756.

Fisher, O.J., Watson, N.J., Escrig, J.E., Witt, R., Porcu, L., Bacon, D., Rigley, M., Gomes, R.L., 2020. Considerations, challenges and opportunities when developing data-driven models for process manufacturing systems. Comput. Chem. Eng. 140, 106881. https://doi.org/10.1016/j.compchemeng.2020.106881.

He, X., Zhu, W., Kwak, H., Yousef, A., Hoteit, H., 2024. Deep learning-assisted Bayesian framework for real-time CO_2 leakage locating at geologic sequestration sites. J. Clean. Prod. 448, 141484. https://doi.org/10.1016/j.jclepro.2024.141484.

Kadlec, P., Gabrys, B., Strandt, S., 2009. Data-driven soft sensors in the process industry. Comput. Chem. Eng. 33, 795–814. https://doi.org/10.1016/j.compchemeng.2008.12.012.

Kim, J., Yu, J., Kang, C., Ryang, G., Wei, Y., Wang, X., 2022. A novel hybrid water quality forecast model based on real-time data decomposition and error correction. Process Saf. Environ. Prot. 162, 553–565. https://doi.org/10.1016/j.psep.2022.04.020.

Kopbayev, A., Khan, F., Yang, M., Halim, S.Z., 2022. Gas leakage detection using spatial and temporal neural network model. Process Saf. Environ. Prot. 160, 968–975. https://doi.org/10.1016/j.psep.2022.03.002.

Leveson, N.G., Stephanopoulos, G., 2014. A system-theoretic, control-inspired view and approach to process safety. AIChE J. 60, 2–14. https://doi.org/10.1002/aic.14278.

Liu, H., Yin, S., Chen, C., Duan, Z., 2020. Data multi-scale decomposition strategies for air pollution forecasting: a comprehensive review. J. Clean. Prod. 277, 124023. https://doi.org/10.1016/j.jclepro.2020.124023.

Liu, N., Wang, J., Sun, S., Li, C., Tian, W., 2022. Optimized principal component analysis and multi-state Bayesian network integrated method for chemical process monitoring and variable state prediction. Chem. Eng. J. 430, 132617. https://doi.org/10.1016/j.cej.2021.132617.

Liu, Y., Jia, M., Xu, D., Yang, T., Yao, Y., 2024. Physics-guided graph learning soft sensor for chemical processes. Chemometr. Intell. Lab. Syst. 249, 105131. https://doi.org/10.1016/j.chemolab.2024.105131.

Liu, Z., Cui, Z., Wang, M., Liu, B., Tian, W., 2024. A machine learning proxy based multi-objective optimization method for low-carbon hydrogen production. J. Clean. Prod. 445, 141377. https://doi.org/10.1016/j.jclepro.2024.141377.

Mkrtchyan, L., Straub, U., Giachino, M., Kocher, T., Sansavini, G., 2022. Insurability risk assessment of oil refineries using Bayesian Belief Networks. J. Loss Prev. Process. Ind. 74, 104673. https://doi.org/10.1016/j.jlp.2021.104673.

Oloruntoba, A., Zhang, Y., Hsu, C.S., 2022. State-of-the-Art review of Fluid catalytic cracking (FCC) catalyst regeneration intensification technologies. Energies 15, 2061. https://doi.org/10.3390/en15062061.

Perera, Y.S., Ratnaweera, D.A.A.C., Dasanayaka, C.H., Abeykoon, C., 2023. The role of artificial intelligence-driven soft sensors in advanced sustainable process industries: a critical review. Eng. Appl. Artif. Intell. 121, 105988. https://doi.org/10.1016/j.engappai.2023.105988.

Qin, R., Zhao, J., 2022. Adaptive multiscale convolutional neural network model for chemical process fault diagnosis. Chin. J. Chem. Eng. 50, 398–411. https://doi.org/10.1016/j.cjche.2022.10.001.

Sharma Timilsina, M., Sen, S., Uprety, B., Patel, V.B., Sharma, P., Sheth, P.N., 2024. Prediction of HHV of fuel by machine learning algorithm: interpretability analysis using Shapley additive explanations (SHAP). Fuel 357, 129573. https://doi.org/10.1016/j.fuel.2023.129573.

Sun, Q., Ge, Z., 2021. A survey on deep learning for data-driven soft sensors. IEEE Trans. Ind. Inf. 17, 5853–5866. https://doi.org/10.1109/TII.2021.3053128.

Wang, X., Qi, X., Zhang, Y., 2024. Deep learning with local spatiotemporal structure preserving for soft sensor development of complex industrial processes. Appl. Soft Comput. 164, 111974. https://doi.org/10.1016/j.asoc.2024.111974.

Wu, W., Song, C., Zhao, J., Wang, G., 2024. Knowledge-enhanced distributed graph autoencoder for multiunit industrial plant-wide process monitoring. IEEE Trans. Ind. Inf. 20, 1871–1883. https://doi.org/10.1109/TII.2023.3280935.

Xue, P., Zhang, M., Wang, K., Feng, D., Liu, H., Liang, C., Jiao, F., Gong, H., Xu, X., Wang, Z., 2024. How hydrothermal factors and CO_2 concentration affect vegetation carbon sink over time and elevation gradient. J. Clean. Prod. 449, 141800. https://doi.org/10.1016/j.jclepro.2024.141800.

Yuan, X., Qi, S., Shardt, Y.A.W., Wang, Y., Yang, C., Gui, W., 2020. Soft sensor model for dynamic processes based on multichannel convolutional neural network. Chemometr. Intell. Lab. Syst. 203, 104050. https://doi.org/10.1016/j.chemolab.2020.104050.

Yuzgec, U., Dokur, E., Balci, M., 2024. A novel hybrid model based on Empirical Mode Decomposition and Echo State Network for wind power forecasting. Energy 300, 131546. https://doi.org/10.1016/j.energy.2024.131546.

Zhang, B., Cheng, S., Zhao, Y., Lu, F., 2024. Health impacts of spatiotemporal variation in PM2.5 concentrations from heavy-duty diesel trucks in Beijing. J. Clean. Prod. 434, 140025. https://doi.org/10.1016/j.jclepro.2023.140025.

Zhang, D., Dai, Y., Chen, K., Guo, A., Liu, H., Wang, Z., 2021. Agglomeration of solid particles in fluidized catalytic cracking slurry oil: particle separation by the Oil–Water interface and particle composition analysis. Energy & Fuels 35, 3219–3227. https://doi.org/10.1021/acs.energyfuels.0c03705.